Low-frequency acoustic atomization with oscillatory flow around micropillars in a microfluidic device

Low-frequency acoustic atomization with oscillatory flow around micropillars in a microfluidic device

Yin Nee Cheung*[a], Nam Trung Nguyen[b], Teck Neng Wong[a]

a School of Mechanical and Aerospace Engineering, Nanyang Technological University, 50 Nanyang Avenue, Singapore 639798, Singapore

*Email: mailccheung@gmail.com

b Queensland Micro- and Nanotechnology Centre, Griffith University, Brisbane QLD 4111, Australia

Abstract:

This letter reports a low frequency acoustic atomization technique with oscillatory extensional flow around micropillars. Large droplets passing through two micropillars are elongated. Small droplets are then produced through the pinch-off process at the spindle-shape ends. As the actuation frequency increases, the droplet size decreases with increasing monodispersity. This method is suitable for in-situ mass production of fine droplets in a multi-phase environment without external pumping. Small particles encapsulation was demonstrated with the current technique.

Acoustic atomization with ultrasound is a useful tool for the production of micron to submicron droplets for food and biomedical applications. The early type atomizer, fountain-type atomizer[1], focuses the acoustic power to the surface of a pool of liquid with specific depth for efficient atomization. The capillary wavelength on the liquid surface decreases with increasing acoustic frequency (10–1000 kHz) and causes a reduction in the droplet size. Another type of ultrasonic atomizer is the single lead zirconium titanate (PZT) element thickness mode piston atomizer.[2] This type of atomizer operates in the early MHz range (1–5 MHz) and is able to produce submicron droplets.

Surface acoustic wave (SAW) atomizer has been proposed for miniaturization and low-power-consumption production of micron to submicron droplets.[3-6] The SAW works in the MHz frequency range (10-500 MHz) and can handle a small fluid volume.[7, 8] The SAW type atomizer is composed of patterned metal interdigitated transducer (IDT) electrodes deposited on a piezoelectric substrate. The SAW waves with amplitudes in the order of nanometers travel along and near the surface of the substrate. The wave is diffracted into a droplet due to the difference of wave propagation speeds in liquid and solid media. Thus, acoustic wave induced inside the droplet generates destabilized capillary waves on the surface of the droplet upon sufficient acoustic excitation. The mechanism for the SAW atomizer is still under active investigation. Several papers have been reported on the possible applications of the device for the generation of different types of small particles.[9–11] Submicron polymeric particles (150-200 nm) were formed through a continuously operating SAW device at a resonance frequency of 8.611 MHz.[9] These large particle aggregates consist of 5-10 nm particles. The biocompatible and degradable nanoparticles are useful for drug deliveryapplications. Similarly, the SAW platform is able to

produce insulin liquid aerosols (3 μm) and solid protein nanoparticles (50-100 nm) at 20 MHz acoustic actuation,[10] as well as multilayer nanoparticles for drug encapsulation.[12]

We propose here a novel microfluidic atomization technique, which is facilitated by the oscillatory extensional flow around micropillars. Oscillatory refers to the back-and-forth motion of the droplet caused by the piezoelectric actuation. Extensional refers to the extensional flow affecting droplet deformation and breakup. Small liquid droplets are generated in an oil medium through the pinch-off of the spindle shaped end of the elongated droplet interface due to the extensional flow between two micropillars. Our current investigation demonstrates a method of small droplet production with several advantages. First, the actuation frequency I low, ranging only from several to tens of Hz. Second, the method allows for in-situ production of small droplets in another immiscible liquid. And third. the device is standalone and does not need external pumping.

Fig. 1 shows the device configuration investigated in this paper. Micropillars with a diameter of 200 μm were fabricated in a microfluidic chamber with a width of 1400 μm. Several aqueous droplets (deionized water, DI) were injected into the chamber before the atomization experiment. DI water was used as the dispersed phase and light mineral oil (M5904, Sigma Aldrich Co.) with 0.7% w/w of Span 80 (S6760, Sigma Aldrich Co.) was used as the continuous phase. Span 80 was used to reduce the interfacial tension and to change the wetting property of the oil film separating the droplet and the channel wall. Polydimethylsiloxane (PDMS) and its curing agent (Sylgard 184, Dow Corning Corp.) were mixed in a proportion of 10:1 by weight and used for replicating the microfluidic chamber patterns from an SU-8 mold (SU8-100,

MicroChem Corp.).[13] The PDMS device was cured at 80^{o}C for 2.5 hours and then bonded to a glass slide coated with a thin layer of PDMS. The height of the microfluidic chamber is around 130 μm. A piezoelectric disk with a diameter of 31.8 mm (T216-A4NO-373X, Piezo Systems Inc.) was embedded within the PDMS device using adhesive spacers. The PDMS membrane between the bottom of the piezoelectric disk and the top of the microfluidic chamber has a thickness of around 1.1 mm. The piezoelectric disk was actuated by sinusoidal waveforms from a signal generation unit that included a signal generator (AFG320, Tektronix Inc.) and a power amplifier (790 Series, PCB Piezotronics Inc.). Low-frequency sinusoidal actuation causes a back-and-forth fluid flow around the micropillars. Images of the droplet formation process were captured using a high-speed camera (FASTCAM-APX RS, Photron Inc.) attached to an inverted microscope (Eclipse Ti, Nikon Ltd.). The images were processed using the open source image software ImageJ.[14]

Fig. 2(a) and (b) show the droplet atomization trajectories that were captured at 10 frames per second (fps). Droplet pinch-off resembling the case in surfactant-mediated tip-streaming[15] was observed when the droplet elongated with spindle ends between two micropillars. The size of the formed droplet decreases with increasing acoustic frequency. Fig. 2(c) shows the representative moment of pinch-off. Droplets formed at 30 Hz were smaller than those formed at 20 Hz. Figure 3(a) shows the typical droplet deformation and the pinch-off process of the interface. The droplet was first stretched by the non-uniform extensional flow between the micropillars. Instability developed at the deformed droplet interface leading to the formation of the small droplets.

The flow across micropillars array can be analyzed based on the porous media approach. The pressure drop through the array is related to the volume averaged (superficial) velocity as[16-17] $-dP/dx = (\mu/K)U_s$, where P is the pressure, μ is the liquid viscosity and K is the permeability of the medium and U_s is the superficial velocity. Considering fluid flow through a confined porous medium, an additional term is required to satisfy the no-slip boundary condition on the walls $-dP/dx = (\mu/K)U_s + \mu_{eff}\, d^2U_s/dy^2$, where μ_{eff} is the effective viscosity.[16, 18] Another important consideration is the geometric parameters of the micropillars array (x_p, y_p, d_p) which affect the permeability K and thus the flow through the media.[17, 19-20] Droplet breakup occurs when the capillary number, Ca, reaches the critical capillary number, Ca_{cr}. The capillary number is defined as[21] $Ca = U\mu_c/\sigma = \dot{\gamma}R\mu_c/\sigma = \dot{\varepsilon}R\mu_c/\sigma$, where U is the velocity, σ is the interfacial tension, μ_c is the viscosity of the continuous phase, R is the maximum radius of the droplet that do not break, $\dot{\gamma}$ is the shear rate, $\dot{\varepsilon} = du(x)/dx$ is the extension rate and $u(x)$ is the velocity distribution for fluid flowing through the micropillars. The interfacial tension between DI water and mineral oil with 0.7% w/w of Span 80 was measured as 4.46 mN/m using a tensiometer (FTA200, First Ten Ångstroms, Inc.). The viscosity of the mineral oil was measured as 26.45 mPa.s at 25^{o}C using a rheometer (DHR-2, TA Instruments, Inc.).

Droplet deformation, the mode of instability and the critical capillary number Ca_{cr} for droplet breakup depend on the viscosity ratio between the two fluids.[22-26] The viscosity ratio (λ, viscosity of dispersed phase to that of continuous phase) is approximately 0.03 for DI water with a viscosity of 0.89 mPa.s at 25^{o}C. The low viscosity ratio causes the drop to deform into a spindle shape by the extensional flow between the micropillars, Fig. 3(a) and (b). In addition, the

breakup event is time dependent and governed by the properties of the droplet and the entire time history of the velocity gradient that it experienced.[21, 24] The critical capillary number Ca_{cr} of extensional flow is much smaller than that of shear flow. Thus, extensional flow generates smaller droplets.[21, 23]

In contrast to the double tails of a deformed droplet as formed due to shear flow near the side walls in a microchannel according to the experiments conducted by Mulligan and Rothstein,[21] a single tail is formed in the middle of the droplet between two micropillars in our configuration under the extensional flow, Fig. 3(a) and (b). According to the similarity solution for a pressure-driven oscillatory flow in a channel, the real part of the velocity is:[27]

$$u_{real}(y,t)=\frac{c}{b}\cos(\omega t)\left\{\cos\left(\sqrt{\frac{b}{a}}y\right)-\left[\sin\left(\sqrt{\frac{b}{a}}y\right)\Big/\sin\left(\sqrt{\frac{b}{a}}\right)\right]\left[\cos\left(\sqrt{\frac{b}{a}}\right)+1\right]-1\right\},$$

where $a=\mu\cos(\omega t)$, $b=\rho\omega\sin(\omega t)$, $c=\rho F_0\left[1+\sin(\omega t)\right]$, F_0 is the amplitude of the applied force, μ is the liquid viscosity, ω is the oscillation frequency and ρ is the liquid density. The oscillatory flow causes non-uniform extensional flow between micropillars. Fig. 3(c) shows the flow around micropillars for mineral oil mixed with 7-μm polystyrene microspheres (35-2B, Thermo Fisher Scientific Inc.). The images were captured with a CCD camera (iXon^{EM}+, Andor Technology Ltd.). Extensional flow occurs between micropillars in both horizontal and diagonal directions. Flows through a single[28] and micropillars array involve complex behaviors like vortex shedding, lateral flow oscillation[29] and versatile flow trajectories (zigzag, laterally displaced and dispersive)[30] are currently under active investigation. The potential application of the our method for small particles encapsulation is demonstrated in Fig. 3(b). Small particles with a nominal

diameter of 3.2 μm (R0300B, Thermo Fisher Scientific Inc.) reside near the droplet surface are encapsulated in the pinched-off droplets.

The size distribution of the droplets was obtained using the ImageJ software.[14] A total of around 500 droplets were analyzed for the different actuation frequencies. The equivalent diameter of each droplet was obtained based on the area values obtained from analysis. Figure 4 shows the size distributions for the actuation frequencies of 5 Hz and 10 Hz. The actuation was turned on for duration of 1 to 2 minutes before droplet images were captured for size analysis. The histogram of 5 Hz actuation shows a broader spectrum than that of the 10 Hz. The standard deviation of the size distribution were measured as 3.7 μm and 2.7 μm at 5 Hz and 10 Hz, respectively. The peak sizes for the two cases are relatively close to each other; e. g. 9 μm for 5 Hz and 8 μm for 10 Hz. As the geometric parameters (x_p, y_p, d_p) of the micropillars array affect the resultant oscillatory flow and its extension rate, the droplet size could be controlled by tuning the parameters of the micropillar to enhance the extension rate for even smaller sizes.

In conclusion, we demonstrate a method for low-frequency acoustic atomization with oscillatory flow around micropillars in a microfluidic device. Extensional flow between micropillars causes the droplet to deform with a spindle shaped end and thus facilitating the formation of small droplets. The process resembles the surfactant mediated tip-streaming phenomenon. Fluids with a low viscosity ratio also facilitate the formation of the spindle shaped end during the formation process. Droplet size decreases with increasing actuation frequency. The novel method proposed here is suitable for in-situ production of small droplets in a microfluidic environment.

The authors would like to acknowledge Prof. Haiqing Gong for use of his microscope and high speed camera. The authors gratefully acknowledge research support from the Singapore Ministry of Education Academic Research Fund Tier 2 research grant MOE2011-T2-1-036.

1. R. J. Lang, J. Acoust. Soc. Am. **34**, 6 (1962).
2. G. Forde, J. Friend, and T. Williamson, Appl. Phys. Lett. **89**, 064105 (2006).
3. M. Kurosawa, T. Watanabe, and T. Higuchi, in Proceedings of the IEEE Micro Electro Mechanical Systems: An Investigation of Micro Structures, Sensors, Actuators, Machines and Systems, Amsterdam, the Netherlands, 29 January-2 February 1995 (IEEE, 1995), pp. 25-30.
4. M. Kurosawa, T. Watanabe, A. Futami, and T. Higuchi, Sensor. Actuat. A-Phys. **50**, 69 (1995).
5. M. Kurosawa, A. Futami, and T. Higuchi, in Transducers' 97: Proceedings of 1997 International Conference on Solid-State Sensors and Actuators, Chicago, Illinois USA, 16-19 June 1997 (IEEE, 1997), pp. 801-804.
6. K. Chono, N. Shimizu, Y. Matsui, J. Kondoh, and S. Shiokawa, Jpn. J. Appl. Phys. **43**, 2987 (2004).
7. M. Alvarez, J. Friend, L. Yeo, and D. Arifin, in Proceedings of the 16th Australasian Fluid Mechanics Conference, Gold Coast, Australia, 3-7 December 2007, edited by P. Jacobs, T. McIntyre, M. Cleary, D. Buttsworth, D. Mee, R. Clements, R. Morgan, and C. Lemckert (School of Engineering, The University of Queensland, Brisbane, 2007), pp. 621-624.

8. A. Qi, L. Y. Yeo, and J. R. Friend, Phys. Fluid **20**, 074103 (2008).

9. J. R. Friend, L. Y. Yeo, D. R. Arifin, and A. Mechler, Nanotechnology **19**, 145301 (2008).

10. M. Alvarez, J. Friend, and L. Y. Yeo, Nanotechnology **19**, 455103 (2008).

11. A. Qi, J. R. Friend, L. Y. Yeo, D. A. V. Morton, M. P. McIntosh, and L. Spiccia, Lab Chip **9**, 2184 (2009).

12. P. Chan, A. Qi, Semper, A. Rajapaksa, J. Friend, and L. Yeo, in μTAS 2012: Proceedings of 16th International Conference on Miniaturized Systems for Chemistry and Life Sciences, Okinawa, Japan, 28 October-1 November 2012 (MicroTAS, 2012), pp. 728.

13. J. C. McDonald, D. C. Duffy, J. R. Anderson, D. T. Chiu, H. Wu, O. J. A. Schueller, and G. M. Whitesides, Electrophoresis **21**, 27 (2000).

14. W. S. Rasband, ImageJ, U.S. National Institutes of Health, Bethesda, Maryland, USA, http://imagej.nih.gov/ij/, (1997-2014).

15. S. L. Anna and H. C. Mayer, Phys. Fluids **18**, 121512 (2006).

16. A. Tamayol, N. S. K. Gunda, M. Akbari, S. K. Mitra, and M. Bahrami, in Proceedings of the ASME 2012 10th International Conference on Nanochannels, Microchannels, and Minichannels, Rio Grande, Puerto Rico, 8-12 July 2012 (ASME, 2012), 73199.

17. M. Kaviany, *Principles of Heat Transfer in Porous Media* (Springer, 1995).

18. H. C. Brinkman, Appl. Sci. Res. **A1**, 27 (1949).

19. A. Tamayol and M. Bahrami, Int. J. Heat Mass Tran. **52**, 2407 (2009).

20. A. Tamayol and M. Bahrami, Phys. Rev. E **83**, 046314 (2011).

21. M. K. Mulligan and J. P. Rothstein, Phys. Fluids **23**, 022004 (2011).

22. G. I. Taylor, Proc. R. Soc. Lond. A **146**, 501 (1934).

23. B. J. Bentley and L. G. Leal, J. Fluid Mech. **167**, 241 (1986).

24. W. J. Milliken and L. G. Leal, J. Non-Newton. Fluid **40**, 355 (1991).

25. W. J. Milliken, H. A. Stone, and L. G. Leal, Phys. Fluids **5**, 69 (1993).

26. R. A. de Bruijn, Chem. Eng. Sci. **48**, 277 (1993).

27. A. S. Ziarani and A. A. Mohamad, Microfluid. Nanofluid. **2**, 12 (2005).

28. H. Amini, E. Sollier, M. Masaeli, Y. Xie, B. Ganapathysubramanian, H. A. Stone, and D. Di Carlo, Nat. Commun. 4, 1826 (2013).

29. A. Renfer, M. K. Tiwari, F. Meyer, T. Brunschwiler, B. Michel, and D. Poulikakos, Microfluid. Nanofluid. **15**, 231 (2013).

30. R. Quek, D. V. Le, and K.-H. Chiam, Phys. Rev. E **83**, 056301 (2011).

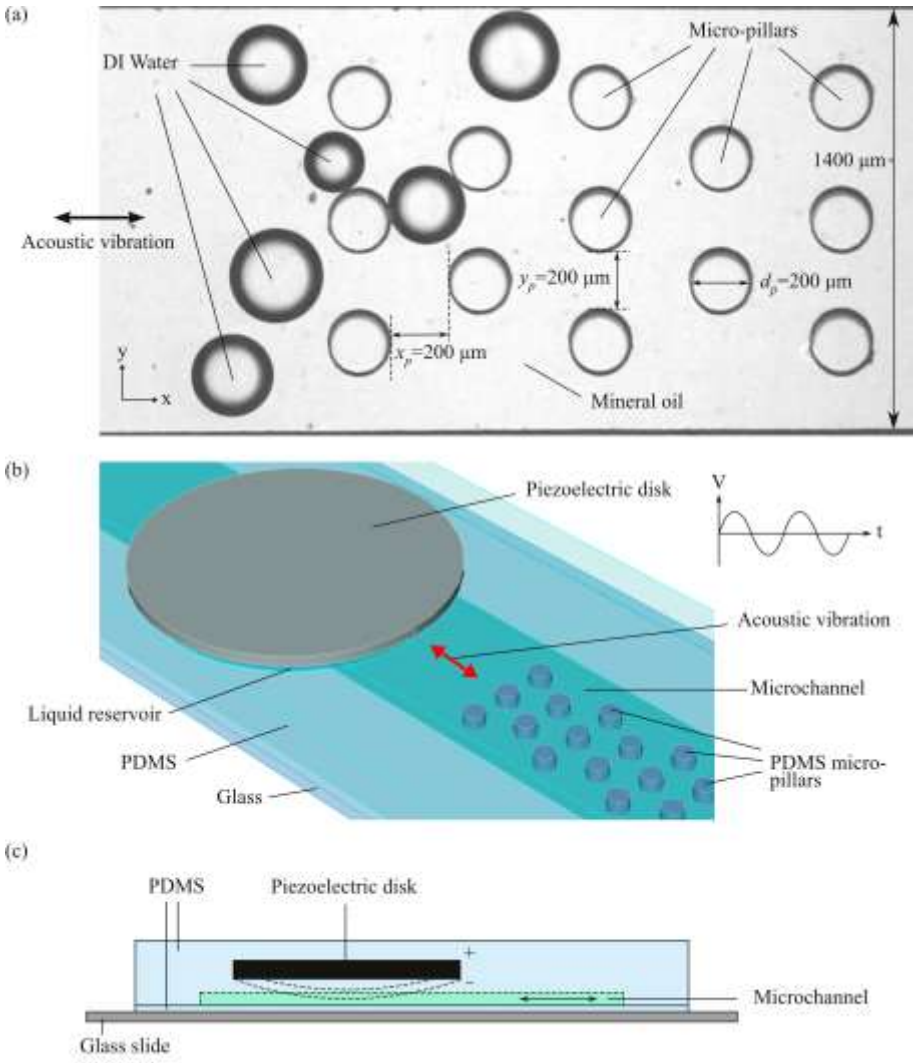

Fig. 1 Device configurations: (a) An array of PDMS micropillars with a diameter of 200 μm in a microfluidic chamber, the double arrow indicates the actuation direction; (b) Sinusoidal actuation from the piezoelectric disk causes a vibrating motion around the micropillars. (c) Cross section of the device.

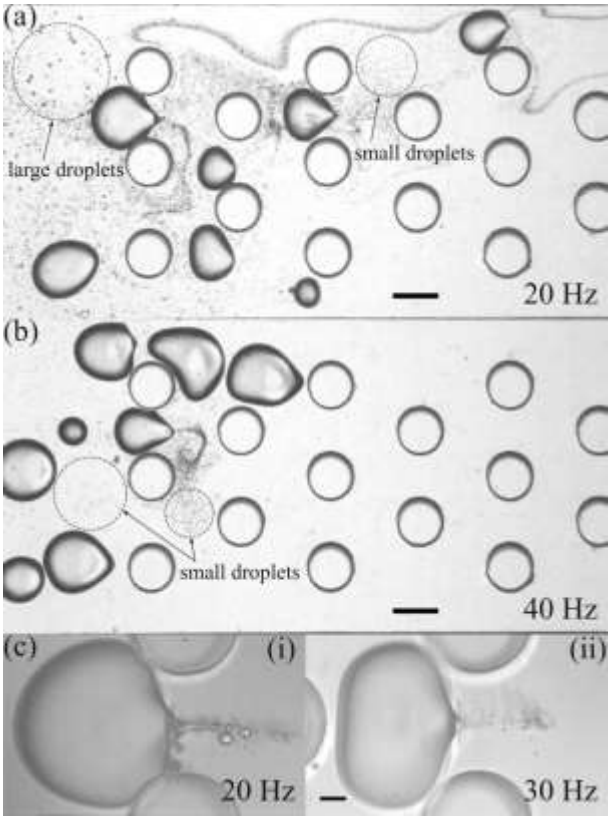

Fig. 2 Droplet atomization around micropillars under a sinusoidal actuation of (a) 20 Hz and ± 109 V (Multimedia view); (b) 40 Hz and ± 142 V. Scale bar for (a) and (b) is 200 μm; (c) Pinch-off process at the spindle shaped end of the elongated droplet between two micropillars; (i) 20 Hz and ± 134 V; (ii) 30 Hz and ± 139 V, scale bar is 50 μm.

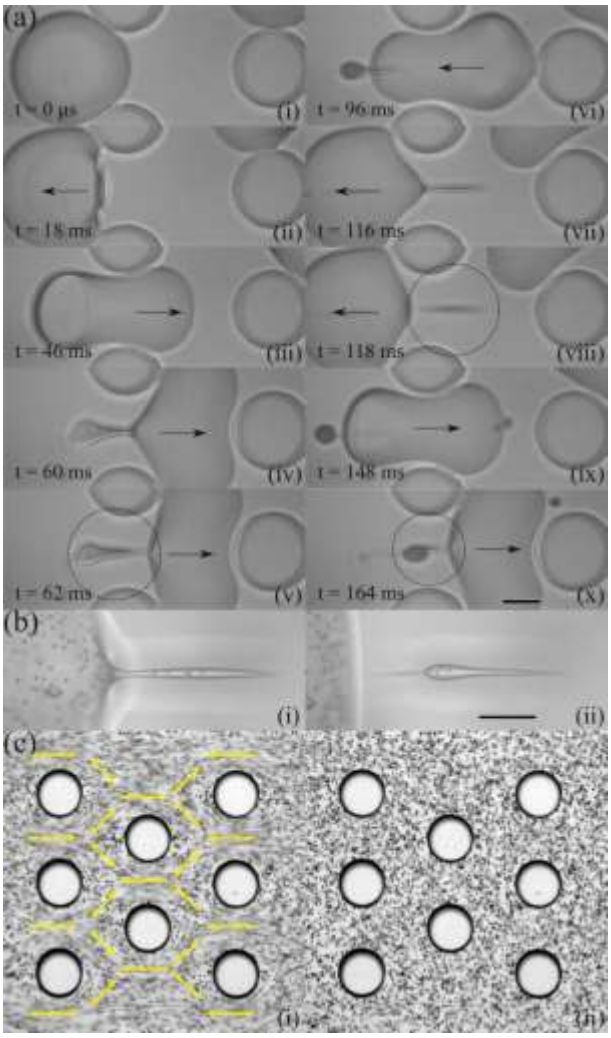

Fig. 3(a) Formation of small droplets as the mother droplet oscillates between the micropillars and causes droplet pinch-off (as circled). The flow is actuated at 10 Hz, ± 117 V, the motion direction of the mother droplet is indicated by the arrow. Scale bar is 100 μm; (b) Demonstration of encapsulation of 3.2 μm polystyrene microspheres (R0300B, Thermo Fisher Scientific Inc.) at 20 Hz and ± 134 V. Scale bar is 50 μm; (c) Mineral oil with 7-μm tracing particles (35-2B, Thermo Fisher Scientific Inc.) undergoes acceleration (Fig. 3(c)(i)) and deceleration (Fig. 3(c)(ii)) during the sinusoidal actuation.

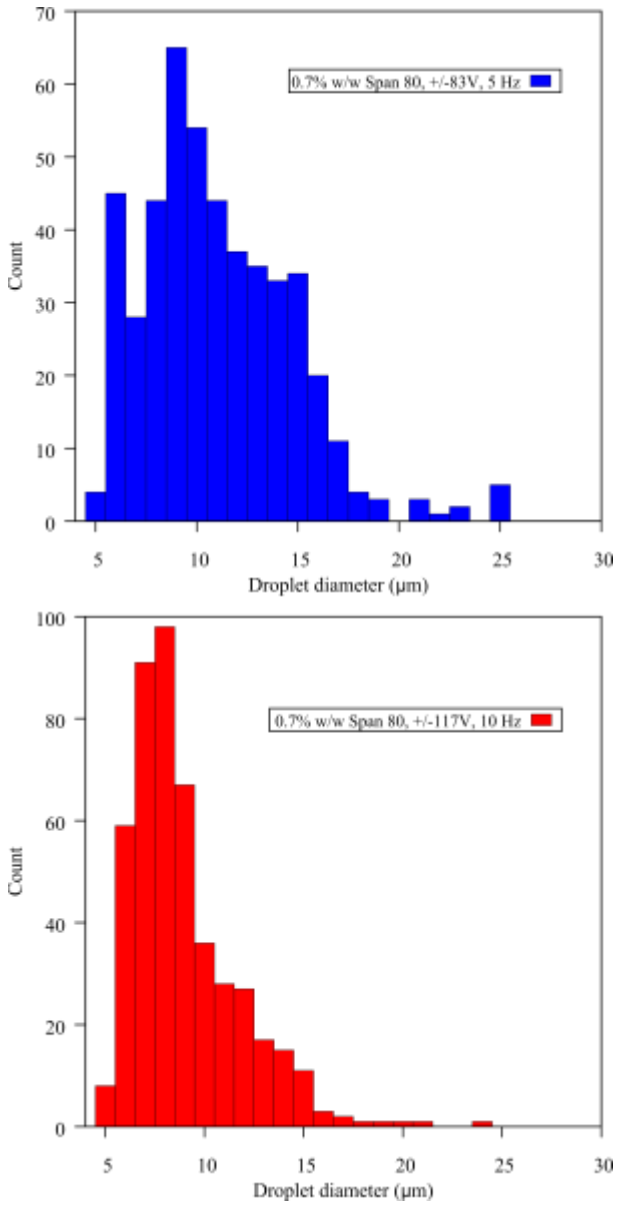

Fig. 4 Count distribution for droplet size under actuation conditions of (a) 5 Hz and ± 83 V; (b) 10Hz and ± 117 V.